Emission of energetic protons from relativistic intensity laser interaction with a cone-wire target

B. S. Paradkar,[1] T. Yabuuchi,[2] H. Sawada,[1] D. P. Higginson,[1] A. Link,[3] M. S. Wei,[4] R. B. Stephens,[4]
S. I. Krasheninnikov,[1] and F. N. Beg[1]
[1]*University of California–San Diego, La Jolla, California 92093, USA*
[2]*Osaka University, Osaka 565-0871, Japan*
[3]*Lawrence Livermore National Laboratory, Livermore, California 94550, USA*
[4]*General Atomics, San Diego, California 92123, USA*
(Received 20 August 2012; published 21 November 2012)

Emission of energetic protons (maximum energy ∼18 MeV) from the interaction of relativistic intensity laser with a cone-wire target is experimentally measured and numerically simulated with hybrid particle-in-cell code, LSP [D. R. Welch *et al.*, Phys. Plasmas **13**, 063105 (2006)]. The protons originate from the wire attached to the cone after the OMEGA EP laser (670 J, 10 ps, 5×10^{18} W/cm^2) deposits its energy inside the cone. These protons are accelerated from the contaminant layer on the wire surface, and are measured in the radial direction, i.e., in a direction transverse to the wire length. Simulations show that the radial electric field, responsible for the proton acceleration, is excited by three factors, viz., (i) transverse momentum of the relativistic fast electrons beam entering into the wire, (ii) scattering of electrons inside the wire, and (iii) refluxing of escaped electrons by "fountain effect" at the end of the wire. The underlying physics of radial electric field and acceleration of protons is discussed.

DOI: 10.1103/PhysRevE.86.056405 PACS number(s): 52.57.Kk, 52.65.Pp

I. INTRODUCTION

The remarkable progress in the development of high intensity lasers in the past two decades has opened up exciting opportunities in the field of high energy density physics (HEDP). The laser-matter interaction experiments at relativistic intensities ($\geqslant 10^{18}$ W/cm^2) allow one to explore properties of matter under the extreme conditions, relevant to laboratory astrophysics [1–3], fast ignition concept of inertial confinement fusion [4,5] and compact particle accelerators [6]. One such experiment is guiding of relativistic electrons, carrying extremely high current densities ($\sim 10^{12}$ A/cm^2), by a cone-wire target. Such targets have experimentally [7,8] demonstrated the guiding of relativistic fast electrons, generated from the interaction of short pulse laser with a hollow cone, by a wire attached to it. The cone-wire targets are also used to study the issues relevant to the scheme of cone-guided fast ignition [5]. Particularly, the underlying physics of coupling of the laser energy to the fast electrons can be effectively studied using these targets [9,10].

The guiding of electrons in cone-wire targets is achieved by the combined effects of radial electric field and azimuthal magnetic field present around the wire. Particle-in-cell (PIC) simulations [7] have demonstrated that the confinement of fast electrons is due to the balancing of outward force by the magnetic field with the inward pull by the radial electric field. This guiding of the fast electrons along the wire surface results in surface heating of the wire by the induced returned current from the background plasma [8]. The expansion of plasma around the cone-wire target was measured experimentally using interferometry [8]. This indicates that the energy from fast electrons is eventually transferred to energetic ions through the excitation of sheath electric field around the wire [11]. The energetic protons from such targets were measured and transient behavior of the radial electric field was diagnosed on the basis of "time of flight" estimates for these protons [12]. It was shown that these expanding protons result in the exponential decay of the electric field in ∼3 ps. Note that the laser pulse duration for this experiment was ∼0.75 ps. Clearly, the study of such energetic protons from the cone-wire targets could provide important information to understand the dynamics of the fast electrons inside the wire.

In this paper, we present a detailed investigation of such proton emission observed with a laser pulse of duration 10 ps. Earlier experiments [12] on proton emission from such targets were carried out in a regime where the laser pulse duration (∼0.75 ps) was much shorter than the time scale for the expansion of proton or plasma around the wire (∼3 ps). Since the protons extract energy from the electric field and electric field plays an important role in guiding of fast electrons along the wire length, it is possible that the expansion of protons from the wire surface will eventually affect the guiding of fast electrons. This is particularly relevant for our experiment where the laser pulse duration (∼10 ps), i.e., the duration of fast electrons production, is longer than the time scale in which the most energetic protons respond to the electric field. Therefore, it is important to investigate the underlying physics of excitation of radial electric field and the proton emission in order to understand the guiding of these fast electrons. In particular, understanding various physical processes which contribute to the excitation of this electric field is crucial to estimate the time scales for which these electric fields are sustained, even in the presence of expanding protons. We have addressed this issue by performing detailed numerical modeling of the experiment incorporating expansion of protons from the wire surface. The emission of protons is numerically modeled with the hybrid PIC code, LSP [13–15]. The excitation of the radial electric field, responsible for the proton acceleration, is studied in detail. We demonstrate that the electric field generation is mainly due to three factors: (i) divergence of the electron beam entering into the wire, (ii) scattering of electrons inside the wire, and (iii) the electrons refluxing at the end of the wire by the so-called "fountain effect" [16,17]. The physics of these

processes and its implication on guiding of fast electrons will be discussed in this paper.

The paper is organized as follows: Section II describes the experimental setup and the observations. Details of numerical modeling are given in Sec. III A and the results of simulations along with the discussion of the physics of proton emission and the radial electric field excitation are given in Sec. III B. Finally conclusions are presented in Sec. IV.

II. EXPERIMENTAL OBSERVATIONS

The experiment was conducted on the OMEGA EP [18] laser facility at the Laboratory for Laser Energetics. The schematic of the experiment is shown in Fig. 1. A Cu wire (40 μm diameter, 1 mm long) was attached to the tip of the Au cone (cone opening angle of 40°, 1 mm long and 20 μm thick wall). The OMEGA EP laser (670 J, 10 ps) was focused into this cone to generate relativistic fast electrons. The intensity of the laser was $\sim 5 \times 10^{18}$ W/cm^2. In addition, another laser pulse (300 J, 1 ps) was used to produce backlighter protons (from a separate foil) to image electromagnetic fields around the cone and wire. The fast electrons escaping axially from the wire were measured with a vacuum electron spectrometer [on the laser (i.e., wire) axis], whereas the transversely emitted energetic protons, both from the wire and backlighter laser, were diagnosed with a stack of radiochromic films [19] (RCFs) as shown in Fig. 1. Since protons deposit their energy near the Bragg peak [20], each RCF layer captures protons of specific energy with a relatively narrow energy spread. In the experiment, 12 such RCF layers were used which could measure protons in the energy range from 5 to 60 MeV. Interestingly, even when energy of the second laser pulse was very low (~30 J), we found strong signals on RCF images. This indicated that the protons were emitted from the wire, as the backlighter protons number was very low. The two-dimensional image obtained on the RCF layer for such a case is shown below in the inset of Fig. 1. It shows the image

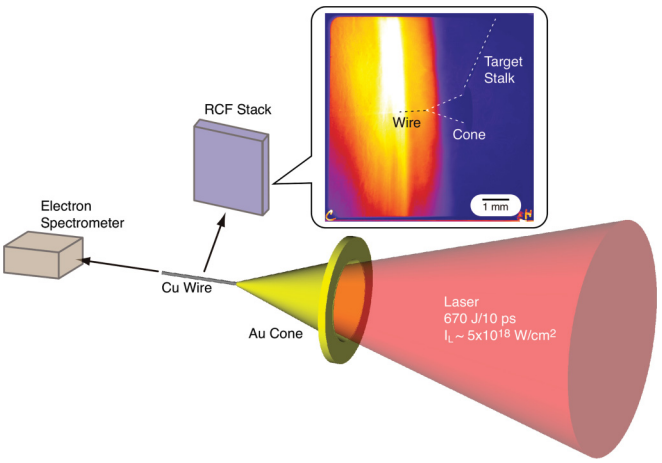

FIG. 1. (Color online) Schematic of the experiment: The OMEGA EP laser was focused into the Au cone. The proton emission from the Cu wire attached to the cone is measured with RCF stacks. The fast electrons escaping axially were diagnosed with a vacuum electron spectrometer. The image on one of the RCF stacks, measuring 9 MeV protons is shown in the inset.

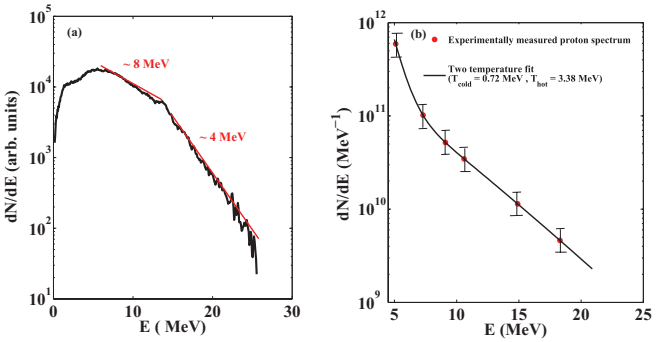

FIG. 2. (Color online) (a) Experimentally measured escaped electrons spectrum. (b) Radial proton spectrum. The slope temperature of fast electrons was found to be in between ~4 and 8 MeV. The black line in (b) shows the two-temperature fit to the experimental data.

from the RCF layer corresponding to the 9 MeV protons. The shadow of the cone tip as well as the cone opening can be clearly seen in this image. This shadow presumably is due to the backlighter protons.

The experimental measurements are shown in Fig. 2. The escaped electrons and the proton spectra are shown in Figs. 2(a) and 2(b), respectively. The proton spectrum shows that protons with a maximum energy of 18 MeV were emitted from the wire in the radial direction. Also, the two-temperature fitting [black line in Fig. 2(b)] of the proton spectrum gives cold temperature, $T_{\rm cold} = 0.72$ MeV, and hot temperature, $T_{\rm hot} = 3.38$ MeV. The measured escaped electrons spectrum shows typical features of the vacuum electrons spectrum reported in the earlier experiments [21,22]. The slope temperature of the measured vacuum electrons is in the range of 4–8 MeV (depending upon the selection of the energy window) as can be seen from Fig. 2(a). Note that this temperature is considerably higher than that predicted by ponderomotive scaling [23] (~500 keV) for the corresponding laser intensity of 5×10^{18} W/cm^2. This enhancement in the fast electrons temperature is due to the presence of considerable preformed plasma inside the cone target due to the laser prepulse [24–27]. The estimated energy in the prepulse and amplified spontaneous emission (ASE) in this experiment was ~350 mJ. These measured spectra are used as constraints in the numerical modeling of the experiment to determine the energy of the fast electrons to be injected into the wire. Details of this will be given in the next section. Having described the experiment and the experimental data, we now move to the numerical modeling of the experiment to discuss in detail the physics of the proton emission in the radial direction and the excitation of radial electric field around the wire.

III. NUMERICAL MODELING OF THE EMISSION OF PROTONS FROM THE WIRE

A. Numerical setup for the simulations

The underlying physics of the relativistic intensity laser interaction with the cone-wire target can be broadly divided into two topics, viz., the generation of a relativistic fast electron beam and transport of this beam in the wire. The generation of fast electrons inside such targets is an active area of research. This is mainly due to the fact that the role of preformed plasma

inside the code is not clearly understood. The generated fast electrons then travel through the cone tip to enter the wire. These electrons can be stopped by resistive (Ohmic) electric fields set up by the background return current [10]. In addition, the fast electrons can be lost radially due to the scattering inside the wire. Finally, when the electrons reach the end of the wire, some of them are reflected back by the electrostatic sheath electric fields [9]. All these processes and their interplay with each other make numerical modeling of cone-wire targets fairly complicated.

Full-scale PIC simulations with modeling of laser plasma interaction (LPI) for this experiment are extremely challenging due to the long spatial and temporal scales (target dimension ~mm and laser pulse duration ~10 ps) of the problem. Typically, such large problems can be efficiently handled using a hybrid approach where the target is treated as a fluid background and the transport of the relativistic fast electrons, generated from LPI, is modeled by injecting "kinetic" electrons into this fluid background [28]. In this treatment, although there are uncertainties about the distribution function of the injected fast electrons (due to the absence of the LPI model in the simulations), they can be addressed by checking the robustness of the model by performing the series of simulations with different injected spectra of generated fast electrons. Of course, various details of actual LPI such as laser filamentation, self-focusing [29] are not considered in this approach. But in our case, since the protons are emitted due to the transport of electrons through the wire, we argue that detailed physics of LPI can be neglected in the first-order approximation. Therefore, we have simulated the emission of protons from the wire by modeling the transport of the injected fast electrons through the wire.

We have performed these simulations with an implicit PIC code, LSP [13–15] in R-Z cylindrical symmetric geometry. In our hybrid approach, Cu wire of the exact experimental dimensions (1 mm long and 40 μm diameter) is treated as fluid plasma at solid density and the fast electrons, injected in front of this wire, are considered as kinetic particles. In addition, a contaminant layer with kinetic protons and electrons is added on all the wire surfaces. The uniform grid resolution of 0.25 μm and temporal time steps of $c\Delta t = 0.025$ μm are considered for these simulations. Here, c is the speed of light. The sensitivity of the simulation for the finer grid resolution of 0.1 μm is tested by performing a small time-scale (~1 ps) simulation. The experimentally measured fast electrons spectrum [refer to Fig. 2(a)] is used as a constraint to inject fast electrons into the wire. Thus, the fast electrons with a slope temperature of 8 MeV are injected into the wire in the forward direction, i.e., the direction of laser propagation. The energy in the fast electron beam is taken as 67 J, corresponding to the laser to wire coupling efficiency of 10%. In general, the coupling efficiency depends upon various factors such as laser pulse energy and duration, preformed plasma scale length inside the cone, cone wall material, etc. But for the present studies, we have assumed constant coupling efficiency for simplicity. Here, we want to point out that the chosen value of 10% conversion efficiency is the upper bound on the efficiency [9]. Thus for all the simulations, the total energy of the electron beam entering into the wire is held constant and the physics of radial electric field excitation is studied for different fast electron energy distributions. These electrons are injected into the wire for the duration of laser pulse, i.e., 10 ps (square temporal pulse). The uncertainty in the electron beam divergence is accounted by running simulations with two extreme cases: In the first case, a divergent electron beam with a transverse beam temperature ($\gamma_\perp$) of 1 MeV and parallel temperature (γ_z) of 8 MeV is considered, whereas in the second case, a directed beam with same parallel temperature but negligible transverse beam temperature (10 keV) is simulated. Results of two these cases will be discussed in detail in this section. Also, typically the generated fast electrons spectrum in the laser-solid interaction in the presence of preformed plasma exhibits a two-temperature spectrum [27]. To take this into account, two more simulations with the two-temperature electron beam are performed. In these simulations, the cold temperature, $T_{\rm cold}$, is fixed at 500 keV (predicted by ponderomotive scaling), whereas the hot temperature, $T_{\rm hot}$, is taken as 8 and 4 MeV, respectively [refer to Fig. 2(a)] from the vacuum electron spectra. In addition, fixed ionization of Cu ($Z_i = 6$) is assumed for simplicity. Note that in reality, the ionization state of Cu wire changes dynamically with the passage of the fast electrons through the wire. But these finer details may not affect the physics of proton emission discussed in the paper. With this numerical setup, we now turn our attention to the results of these numerical simulations and discuss the physics of radial field excitation and proton emission from the wire.

B. Results and discussion

We first discuss the case with a divergent electron beam with a transverse beam temperature ($\gamma_\perp$) of 1 MeV and parallel temperature (γ_z) of 8 MeV. Since in this case the electrons enter the wire with sufficient transverse momentum, it is expected that the radial loss of these electrons will set up the radial electric field around the wire. Figure 3 shows the fast electrons density [Figs. 3(a), 3(d), and 3(g)], proton density [Figs. 3(b), 3(e), and 3(h)], and the total electric field around the wire [Figs. 3(c), 3(f), and 3(i)] for the times 3, 8, and 15 ps, respectively. The total electric field is given by $E = \sqrt{E_R^2 + E_Z^2}$, where E_R and E_Z are the radial and axial electric field, respectively. Note that the wire is located between $z = 0$ μm and $z = 1000$ μm. Also, the injection of fast electrons starts from the beginning of simulation, i.e., time = 0 ps. The beam is injected at 10 μm before the start of the wire ($z = 0$ μm). As expected, the loss of electrons in the radial direction due to the transverse of momentum of electrons results in a radial electric field around the wire to which the protons start responding at early times (3 ps). At a later time (8 ps), the protons have expanded considerably thereby forming quasineutral plasma around the wire. This causes a reduction of the radial electric field between $z =$ 500 and 900 μm [Fig. 3(f)]. The simulation also suggests that the standard quasineutral fluid expansion assumption [30] is not valid for maximum energy protons (the protons which are farthest from the wire). This implies that kinetic effects [31] can be important for these protons. We observe the excitation of strong electric field (peak value ~ 0.8 MV/μm) at the end of the wire ($z = 1000$ μm) due to the escape of electrons in the axial direction. This leads to the strong proton emission from

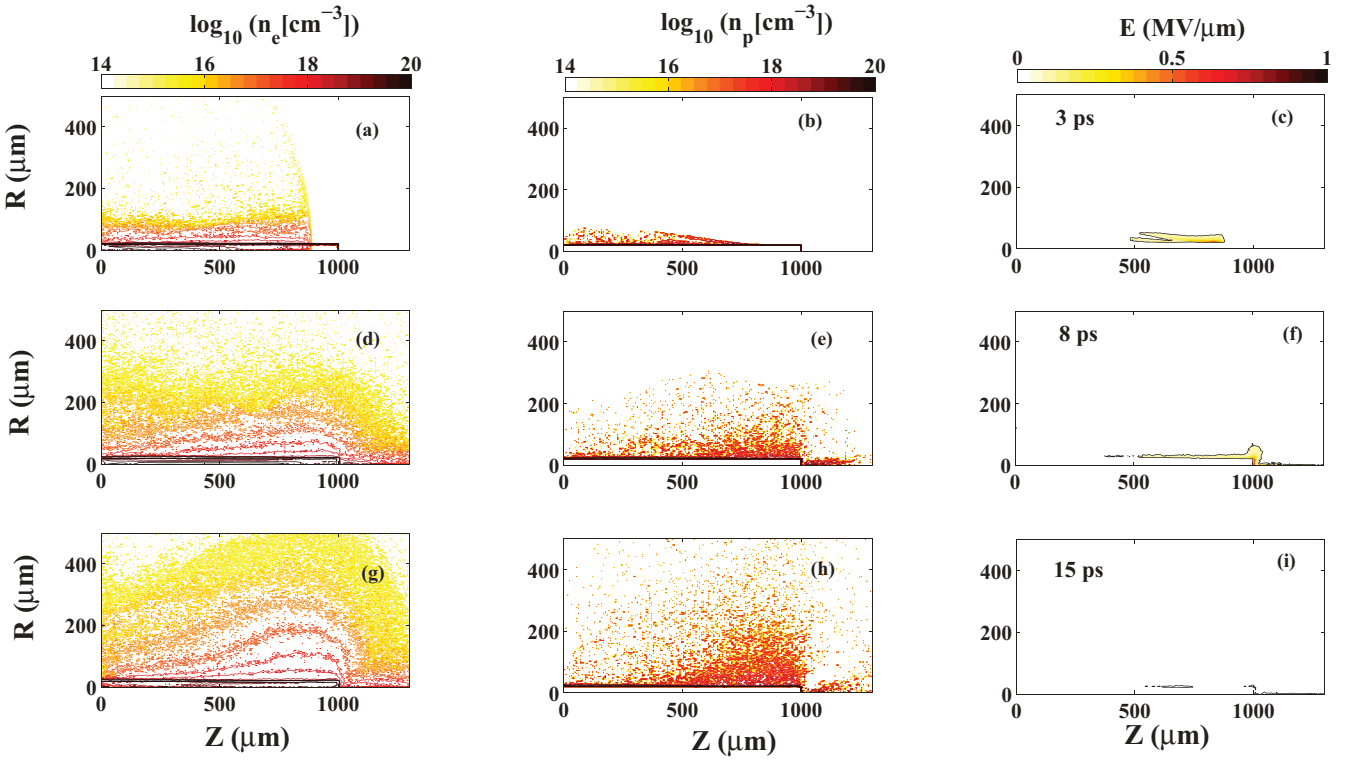

FIG. 3. (Color online) Proton expansion and electric field excitation due to the injection of an electron beam with transverse temperature ($\gamma_\perp$)1 MeV and parallel temperature (γ_z) 8 MeV. Snapshots of fast electron density [(a),(d),(g)], proton density [(b),(e),(h)], and electric field [(c),(f),(i)] at 3, 8, and 15 ps are shown here. The loss of fast electrons in the radial direction results in the excitation of electric field, which causes the proton expansion.

the end of the wire. Finally, the snapshot at 15 ps shows the complete drop offs of electric field by the proton expansion in the vacuum. Note that the injection of fast electrons is stopped at 10 ps. This simulation demonstrates that the transverse momentum of the fast electrons entering into the wire can cause the excitation of the radial electric field around the wire.

Now, we consider the case where the transverse momentum of the beam is negligible and investigate the excitation of the radial electric field around the wire. The simulation results with the directed beam (transverse temperature = 10 keV and parallel temperature = 8 MeV) are presented in Fig. 4. In thiscase, no proton emission from the front end of the wire ($z = 0$ μm) is observed at early times (3 ps) since there are less electrons leaving in the radial direction with transverse momentum compared to Fig. 3(a). But as the electrons propagate further along the wire, some of them exit the wire in the radial direction due to the collisional scattering inside the wire. The radial electric field seen in Fig. 4(c) is due to this effect. We have used standard Spitzer collision frequency in the scattering model [15] incorporated in LSP for these simulations. Finally, similar to the earlier discussed case, we see the excitation of the strong electric field [Fig. 4(f)] at the end of the wire ($z = 1000$ μm) and the quasineutral proton expansion in the radial direction [Figs. 4(e) and 4(h)] as shown in the later time snapshots (8 and 11 ps). To confirm that the electric field observed in Fig. 4(c) (i.e., before the beam electrons leave axially from the other end of the wire) is indeed due to the scattering of the fast electrons inside the wire, we turned off the scattering model in the code and performed a separate simulation for the directed beam.

Thus, with the scattering model "off" and negligible transverse momentum (10 keV) we have eliminated the two sources of radial electric field that we have identified so far. The results of this simulation are presented in Fig. 5. Note that unlike Fig. 4(c), in this simulation the radial electric field is absent [see Fig. 5(c)] due to the negligible loss of fast electrons from the wire during the initial stage [Fig. 5(a)]. This confirms that the scattering of electrons inside the wire contributes to the excitation of the radial electric field. But as the electrons leave from the wire axially at 3.6 ps, a strong electric field [Fig. 5(f)] is observed at the wire end, similar to the cases described earlier. Some of these escaped electrons are refluxed back by the "fountain effect" thereby causing a negative electrons cloud around the wire [Fig. 5(d)]. This results in the setting up of a radial electric field initially near the wire end [Fig. 5(f)]. As these refluxed electrons travel further back (in the $-Z$ direction) we see that the radial electric field is also excited along the length of the wire [Figs. 5(g) and 5(i), respectively] as shown in the 6 ps snapshot. Correspondingly, the protons are emitted predominantly from the end of the wire in this case [Fig. 5(h)]. This simulation demonstrates that the forming of a negative electrons cloud around the wire due to the refluxing of axially escaped electrons also contributes to the excitation of the radial electric field around the wire. Note that this observation of refluxing at the end of the wire is consistent with the recent experiment by Ma *et al.* [9] where

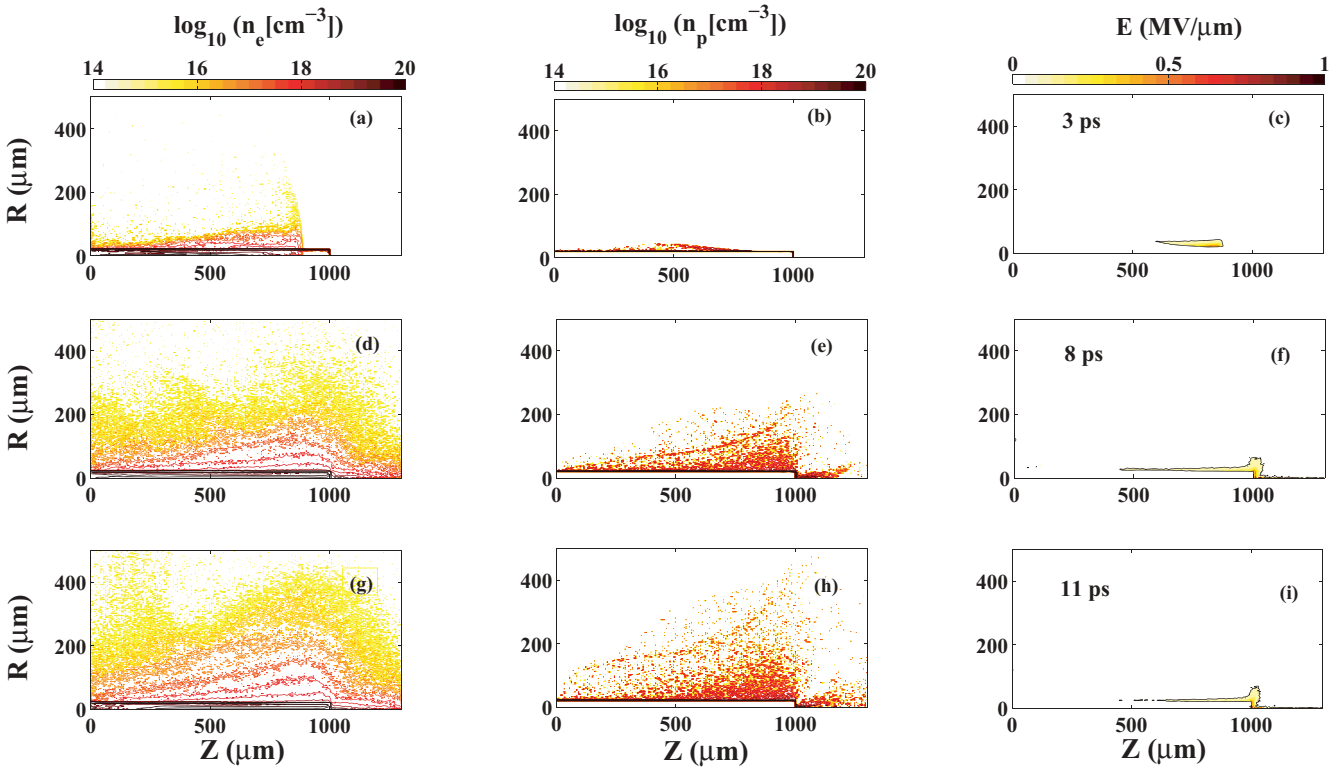

FIG. 4. (Color online) Proton expansion and electric field excitation due to the injection of the electron beam with transverse temperature 10 keV and parallel temperature 8 MeV. The snapshots of fast electron density [(a),(d),(g)], proton density [(b),(e),(h)], and electric field [(c),(f),(i)] at 3, 8, and 11 ps are shown above. The fast electrons with predominantly parallel momentum get scattered inside the wire due to collisions (a). This effect also contributes to the excitation of radial electric field (c) around the wire.

the refluxing of the fast electrons (with temperature $T_{\rm hot}$) was found to be responsible for the bump in the copper $K\alpha$ x-ray emission seen at the end of the wire.

To investigate the effect of injection of the fast electrons beam with two slope temperatures, we performed simulations with the injected electron beam having hot temperatures, $T_{\rm hot}$, of 8 and 4 MeV, respectively. In both cases, the cold temperature, $T_{\rm cold}$, of fast electrons was fixed at ~500 keV, consistent with the ponderomotive scaling [23] at the laser intensity of 5×10^{18} W/cm^2. For simulations, we assume an equal energy partition between the cold and hot electron beams (i.e., 33.5 J each). The total number of electrons escaping axially is calculated by counting all the electrons (time integrated) crossing through the plane at a $Z = 1150\,\mu$m plane with $R \leqslant 20\,\mu$m. We find that there are fewer escaped electrons in the axial direction for the 4 MeV case compared to the 8 MeV case. Accordingly more protons are emitted in the radial direction with 4 MeV fast electrons injection compared to 8 MeV fast electrons injection. Again, consistent with Ref. [9], we observe that a cold beam (500 keV) causes stronger emission of relatively low energy protons (~1–3 MeV) near the cone tip, whereas the hot beam is responsible for proton emission from the wire end ($Z = 1000\,\mu$m). In general, we see that ~1% of the total injected fast electrons energy gets coupled to the radial protons. Although the injection of a two-temperature beam may result in slightly different results quantitatively, depending upon the slope temperature hot tail of the fast electrons distribution, qualitatively the physics of proton emission and radial electric field excitation remains unchanged.

A comparison of the numerically simulated escaped electrons spectrum and radially emitted proton spectrum with the experimental data (presented in Fig. 2) is shown in Figs. 6 and 7, respectively. Note that the escaped electrons spectrum in Fig. 6 is normalized with the total number of escaped electrons for each case. As expected, the slope temperature of the escaped electrons for injection with $T_{\rm hot} = 4$ MeV (solid blue line) is lower than the other simulated cases having the injection with $T_{\rm hot} = 8$ MeV. Also, in Fig. 7 we find that the maximum energy of the radially emitted protons (green dotted curve) for the collimated electrons beam (10 keV transverse temperature and 8 MeV parallel temperature) is ~30 MeV, which is well above the experimentally observed (black solid curve) maximum energy of 18 MeV. This disagreement suggests that the diverging electron beam is necessary to explain the experimentally observed maximum proton energy of 18 MeV (in the framework of our simulations).

Finally, we investigate the question of time scales of a sheath electric field around the wire. As discussed in the Introduction, this electric field plays a crucial role in guiding the fast electrons along the wire surface. In Fig. 8, we have shown the volume integrated radial electric field energy, $\int_V E_r^2\,dV = 2\pi \int_{\substack{R>R_0;\\ 0\leqslant Z\leqslant L}} E_r^2 R\,dR\,dZ$ as a function of time. Here, R_0 and L are the wire radius and length, respectively. Since we have chosen the energy of the fast electron beam to be constant (i.e., constant conversion efficiency) in our simulations, we have plotted the temporal evolution of vacuum radial field energy. Thus, Fig. 8 shows a comparison of the

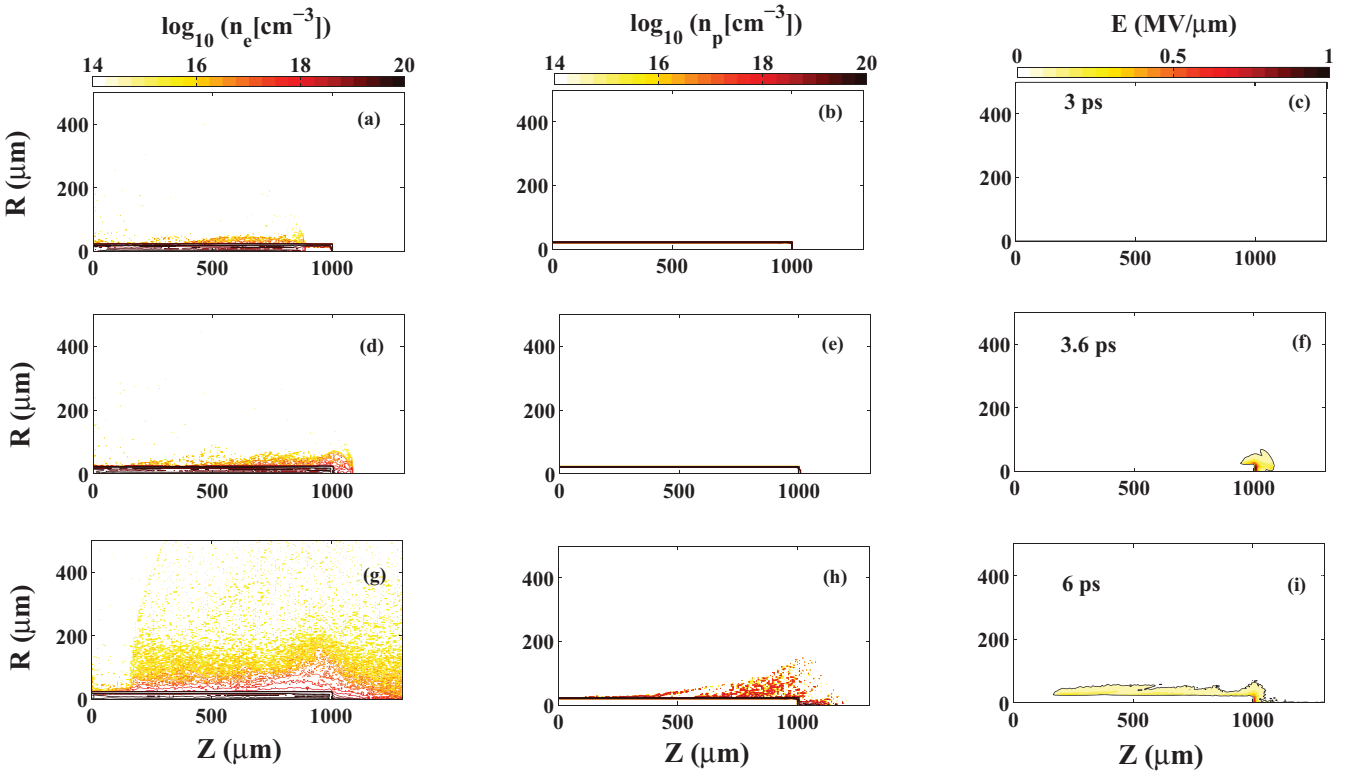

FIG. 5. (Color online) Simulation of transport of directed electron beam (transverse temperature = 10 keV and parallel temperature = 8 MeV) in the absence of scattering of fast electrons inside the wire. The scattering model in the code is turned off for this case. The snapshots of fast electron density [(a),(d),(g)], proton density [(b),(e),(h)], and electric field [(c),(f),(i)] at 3, 3.6, and 6 ps are shown above. Here the excitation of radial electric field is due to the forming of a negative electrons cloud around the wire by refluxing of the axially escaped fast electrons.

temporal evolution of field energy for two different divergences with the same injected beam energy. The beam with higher transverse temperature (1 MeV, red curve) causes a sharper rise of vacuum radial field energy than for the 10 keV transverse temperature case (blue curve). This figure shows that although the field starts decaying after the proton expansion (between 3 and 6 ps), the supply of new electrons, which are coming out of the wire, helps in sustaining the field until the laser pulse in ON. But, clearly this decaying electric field affects the guiding of fast electrons along the surface.

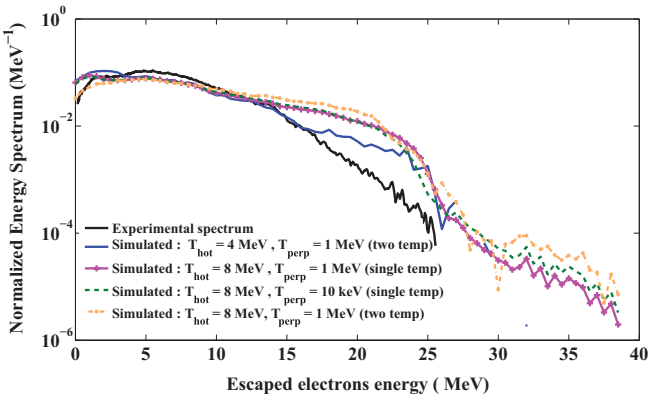

FIG. 6. (Color online) Comparison of the experimentally measured escaped electrons spectrum (black solid line) with the numerically simulated spectra for the various injected electrons distributions. The escaped electrons spectra in the simulations are obtained by counting (time integrated) the electrons passing axially ($R \leqslant 20\ \mu$m) through the extraction plane at $Z = 1150\ \mu$m.

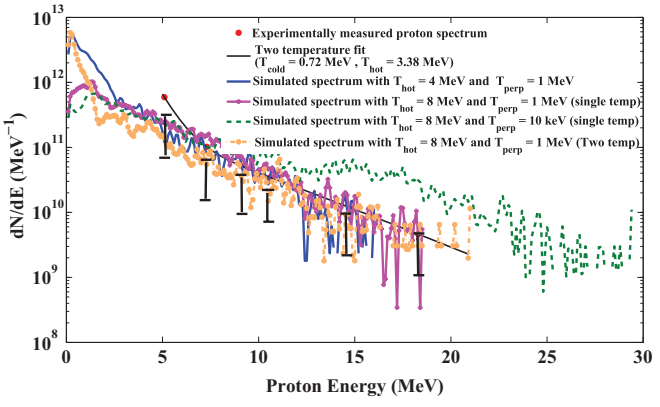

FIG. 7. (Color online) Comparison of the measured radial proton spectrum with the simulated spectra for different injected electrons distributions. Note that the 8 MeV electron beam with the transverse temperature 10 keV (green dotted curve) results in 30 MeV (maximum energy) protons in the radial direction, whereas the experimentally measured (solid black curve) maximum proton energy is ∼18 MeV.

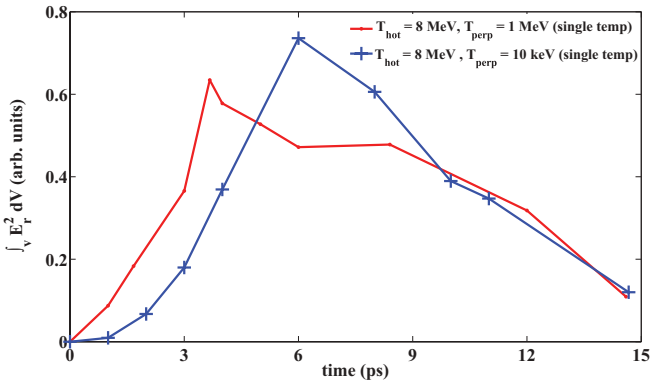

FIG. 8. (Color online) Temporal evolution of volume integrated radial electric field energy around the wire. For the 1 MeV transverse temperature case (red solid line) the energy increases faster than for the directed beam case, i.e., 10 keV transverse temperature (blue curve and "+" marks). The field decays after the protons start expanding (3–6 ps).

IV. CONCLUSIONS

The experimental and numerical investigation of proton emission from the cone-wire target is presented in this paper. Hybrid PIC simulations with the code LSP demonstrate that the radial electric field, responsible for the proton emission, is excited due to three factors: the transverse momentum of fast electrons entering into the wire, collisional scattering of electrons inside the wire, and the formation of a negative electrons cloud around the wire due to the refluxing of escaped fast electrons. At the initial stage of injection of electrons into the wire, the transport is found to be along the wire surface as described in the earlier publications [7,8] but once the protons start expanding into the vacuum the guiding surface electric field reduces. Therefore, quasineutral plasma expansion is observed in the later stages of transport. The modeling shows that inclusion of a proton layer is important while simulating the transport of fast electrons through cone-wire targets, especially when the laser pulse duration is of the order of proton expansion time scale. Finally, measuring such protons can provide useful information about the fast electrons that have entered into the wire. Especially this measurement along with the $K\alpha$ x-ray emission diagnostic [9] and escaped electrons spectrum can be used to estimate the coupling efficiency of laser to the fast electrons (into the wire).

ACKNOWLEDGMENTS

The work was supported by NNSA/U.S. DOE under Contracts No. DE-FG52-09NA29033 (NLUF), No. DE-FC02-04ER54789 (FSC), and No. DE-FG02-05ER54834 (ACE).

[1] D. D. Ryutov, R. P. Drake, J. O. Kane, E. Liang, B. A. Remington, and W. M. Wood-Vasey, Astrophys. J. **518**, 821 (1999).
[2] D. D. Ryutov, B. A. Remington, H. F. Robey, and R. P. Drake, Phys. Plasmas **8**, 1804 (2001).
[3] D. D. Ryutov and B. A. Remington, Phys. Plasmas **10**, 2629 (2003).
[4] M. Tabak, J. Hammer, M. E. Glinsky, W. L. Kruer, S. C. Wilks, J. Woodworth, E. M. Campbell, M. D. Perry, and R. J. Mason, Phys. Plasmas **1**, 1626 (1994).
[5] R. Kodama, P. A. Norreys, K. Mima, A. E. Dangor, R. G. Evans, H. Fujita, Y. Kitagawa, K. Krushelnick, T. Miyakoshi, N. Miyanaga, T. Norimatsu, S. J. Rose, T. Shozaki, K. Shigemori, A. Sunahara, M. Tampo, K. A. Tanaka, Y. Toyama, T. Yamanaka, and M. Zepf, Nature (London) **412**, 798 (2001).
[6] T. Tajima and J. M. Dawson, Phys. Rev. Lett. **43**, 267 (1979).
[7] R. Kodama, Y. Sentoku, Z. L. Chen, G. R. Kumar, S. P. Hatchett, Y. Toyama, T. E. Cowan, R. R. Freeman, J. Fuchs, Y. Izawa, M. H. Key, Y. Kitagawa, K. Kondo, T. Matsuoka, H. Nakamura, M. Nakatsutsumi, P. A. Norreys, T. Norimatsu, R. A. Snavely, R. B. Stephens, M. Tampo, K. A. Tanaka, and T. Yabuuchi, Nature (London) **432**, 1005 (2004).
[8] J. S. Green, K. L. Lancaster, K. U. Akli, C. D. Gregory, F. N. Beg, S. N. Chen, D. Clark, R. R. Freeman, S. Hawkes, C. Hernandez-Gomez, H. Habara, R. Heathcote, D. S. Hey, K. Highbarger, M. H. Key, R. Kodama, K. Krushelnick, I. Musgrave, H. Nakamura, M. Nakatsutsumi, N. Patel, R. Stephens, M. Storm, M. Tampo, W. Theobald, L. Van Woerkom, R. L. Weber, M. S. Wei, N. C. Woolsey, and P. A. Norreys, Nat. Phys. **3**, 853 (2007).
[9] T. Ma, H. Sawada, P. K. Patel, C. D. Chen, L. Divol, D. P. Higginson, A. J. Kemp, M. H. Key, D. J. Larson, S. Le Pape, A. Link, A. G. MacPhee, H. S. McLean, Y. Ping, R. B. Stephens, S. C. Wilks, and F. N. Beg, Phys. Rev. Lett. **108**, 115004 (2012).
[10] J. A. King, K. U. Akli, R. R. Freeman, J. Green, S. P. Hatchett, D. Hey, P. Jamangi, M. H. Key, J. Koch, K. L. Lancaster, T. Ma, A. J. MacKinnon, A. MacPhee, P. A. Norreys, P. K. Patel, T. Phillips, R. B. Stephens, W. Theobald, R. P. J. Town, L. Van Woerkom, B. Zhang, and F. N. Beg, Phys. Plasmas **16**, 020701 (2009).
[11] S. C. Wilks, A. B. Langdon, T. E. Cowan, M. Roth, M. Singh, S. Hatchett, M. H. Key, D. Pennington, A. Mackinnon, and R. A. Snavely, Phys. Plasmas **8**, 542 (2001).
[12] Z. L. Chen, G. R. Kumar, Z. M. Sheng, T. Matsuoka, Y. Sentoku, M. Tampo, K. A. Tanaka, T. Tsutsumi, T. Yabuuchi, and R. Kodama, Phys. Rev. Lett. **96**, 084802 (2006).
[13] D. R. Welch, D. V. Rose, M. E. Cuneo, R. B. Campbell, and T. A. Mehlhorn, Phys. Plasmas **13**, 063105 (2006).
[14] T. P. Hughes, R. E. Clark, and S. S. Yu, Phys. Rev. ST Accel. Beams **2**, 110401 (1999).
[15] D. R. Welch, D. V. Rose, B. V. Oliver, and R. E. Clark, Nucl. Instrum. Methods Phys. Res. A **464**, 134 (2001).
[16] P. Kolodner and E. Yablonovitch, Phys. Rev. Lett. **43**, 1402 (1979).
[17] J. M. Wallace, Phys. Rev. Lett. **55**, 707 (1985).
[18] D. D. Mayerhofer, J. Bromage, C. Dorrer, J. H. Kelly, B. E. Kruschwitz, S. J. Loucks, R. L. McCrory, S. F. B. Morse, J. F. Myatt, P. M. Nilson, J. Qiao, T. C. Sangster, C. Stoeckl, L. J. Waxer, and J. D. Zuegel, J. Phys.: Conf. Ser. **244**, 032010 (2010).

[19] M. Borghesi, D. H. Campbell, A. Schiavi, M. G. Haines, O. Willi, A. J. MacKinnon, P. Patel, L. A. Gizzi, M. Galimberti, R. J. Clarke, F. Pegoraro, H. Ruhl, and S. Bulanov, Phys. Plasmas **9**, 2214 (2002).
[20] A. Caruso and V. A. Pais, Nucl. Fusion **36**, 745 (1996).
[21] A. Link, R. R. Freeman, D. W. Schumacher, and L. D. Van Woerkom, Phys. Plasmas **18**, 053107 (2011).
[22] T. Yabuuchi, B. S. Paradkar, M. S. Wei, J. A. King, F. N. Beg, R. B. Stephens, N. Nakanii, M. Hatakeyama, H. Habara, K. Mima, K. A. Tanaka, and J. T. Larsen, Phys. Plasmas **17**, 060704 (2010).
[23] S. C. Wilks, W. L. Kruer, M. Tabak, and A. B. Langdon, Phys. Rev. Lett. **69**, 1383 (1992).
[24] A. G. MacPhee, L. Divol, A. J. Kemp, K. U. Akli, F. N. Beg, C. D. Chen, H. Chen, D. S. Hey, R. J. Fedosejevs, R. R. Freeman *et al.*, Phys. Rev. Lett. **104**, 055002 (2010).
[25] S. D. Baton, M. Koenig, J. Fuchs, A. Benuzzi-Mounaix, P. Guillou, B. Loupias, T. Vinci, L. Gremillet, C. Rousseaux, M. Drouin *et al.*, Phys. Plasmas **15**, 042706 (2008).
[26] L. Van Woerkom, K. U. Akli, T. Bartal, F. N. Beg, S. Chawla, C. D. Chen, E. Chowdhury, R. R. Freeman, D. Hey, M. H. Key *et al.*, Phys. Plasmas **15**, 056304 (2008).
[27] B. S. Paradkar, M. S. Wei, T. Yabuuchi, R. B. Stephens, M. G. Haines, S. I. Krasheninnikov, and F. N. Beg, Phys. Rev. E **83**, 046401 (2011).
[28] B. S. Paradkar, M. S. Wei, T. Yabuuchi, R. B. Stephens, J. T. Larsen, and F. N. Beg, Plasma Phys. Controlled Fusion **52**, 125003 (2010).
[29] G. Sun, E. Ott, Y. Lee, and P. Guzdar, Phys. Fluids **30**, 526 (1987).
[30] P. Mora, Phys. Rev. Lett. **90**, 185002 (2003).
[31] P. Mora and T. Grismayer, Phys. Rev. Lett. **102**, 145001 (2009).